

APPARENT NON-COEVALITY AMONG THE STARS IN UPPER SCORPIO: RESOLVING THE PROBLEM USING A MODEL OF MAGNETIC INHIBITION OF CONVECTION

James MacDonald and D. J. Mullan

Dept. of Physics and Astronomy, University of Delaware, Newark, DE 19716, USA

Abstract

Two eclipsing binaries in the USco association have recently yielded precise values of masses and radii for 4 low-mass members of the association. Standard evolution models would require these dM4.5-dM5 stars to have ages which are younger than the ages of more massive stars in the association by factors which appear (in extreme cases) to be as large as ~ 3 . Are the stars in the association therefore non-coeval? We suggest that the answer is No: by incorporating the effects of magnetic inhibition of convective onset, we show that the stars in U Sco can be restored to coevality provided that the 4 low-mass member stars have surface fields in the range 200-500 G. Fields of such magnitude have already been measured on the surface of certain solar-type stars in young clusters: if such fields could be measured in low-mass U Sco stars, they might help to discriminate between different approaches which have been suggested for modeling magneto-convection.

1. Introduction

1.1. Star clusters: the importance of coevality

In astrophysics, the determination of a reliable age for a star is a pre-requisite for reliably interpreting the physical parameters of the star. The principal method for determining the age of a star is to assign it to a cluster for which a Hertzsprung-Russell diagram (HRD) can be constructed, and a main sequence turn-off can be identified. However, this method relies on the fundamental assumption of coevality, i.e. all stars in the cluster have the same age. If an example of a non-coeval cluster could be reliably demonstrated, then the basis for many stellar age determinations could be seriously undermined.

A case in point is the Upper Scorpio association (U Sco). In recent years, claims of non-coevality among the stars of U Sco have been published. In this paper, we examine these claims and ask: is it possible to restore the fundamental property of coevality? In the next sub-section, we summarize some of the relevant results which have led a number of research groups to the conclusion of non-coevality.

1.2. The age(s) of stars in U Sco

From photometry of a sample of mainly B stars, de Greus, de Zeeuw & Lub (1989) determined an age of 5 to 8 Myr for U Sco, based on stellar evolutionary models of Maeder (1981). Preibisch et al. (2002), in addition to the main sequence and post main sequence massive stars, studied a large sample of low mass pre-main sequence stars and found a common age of 5 Myr. More recently, Pecaute et al. (2012) analyzed the F stars in the Upper Scorpius, Upper Centaurus–Lupus and Lower Centaurus–Crux subgroups of the Scorpius–Centaurus OB association. They found the U Sco F star luminosities to be a factor of ~ 2.5 lower than predicted by four sets of evolutionary tracks for a 5 Myr old population. Since the stars are on pre-main sequence tracks, a lower luminosity corresponds to an older age. To quantify this, Pecaute et al re-examined the isochronal ages for the U Sco B, A, and G stars, as well as the M supergiant Antares, and determined a mean age of 11 ± 3 Myr, i.e. older by a factor of ~ 2 than the common age reported by

Preibisch et al. (2002). An even younger age has been proposed by Herczeg & Hillenbrand (2015): based on comparison with the β Pic moving group, they conclude that the low mass stars in U Sco must have a mean age of ~ 4 Myr. Rizzuto et al. (2016) determined the age and component masses for seven G- to M-type binary systems in U Sco using the orbital solutions and HST multi-band photometry. They find that their G-type binaries have ages of ~ 11.5 Myr, consistent with the age estimate of Pecaut et al. (2012). However, once again, Rizzuto et al find that their M-type binaries are significantly younger than the G-type binaries: The M-type binaries are found to have ages of ~ 7 Myr. Rizzuto et al note that this age discrepancy corresponds to the following features: the models are found to *under*-predict the luminosity of the M-type stars by 0.8–0.15 dex, or equivalently, the models are found to *over*-predict the effective temperature of the M-type stars by 100–300 K.

Thus there seems to be an inconsistency between the U Sco age which is determined using massive stars and the age which is determined using low-mass stars. In the most extreme cases, the inconsistency between the youngest age (~ 4 Myr) and the oldest age (~ 11.5 Myr) is almost as large as a factor of 3. If these ages are taken literally, then the sense of the inconsistency is such that the *high*-mass stars in U Sco formed first (11.5 Myr ago), and then the *low*-mass stars formed later, perhaps as much as 7 Myr later. This would be hard to understand in terms of star formation: it is more likely that formation of low-mass stars would occur at earlier times, because once a massive star forms in an interstellar cloud, the associated ionization and turbulence “brings an end to most star formation” (Herbig 1962). That is, in a given cloud, massive stars inhibit the subsequent formation of low-mass stars. If sequential star formation is to have a chance of occurring, it should be the low-mass stars that form first, followed at a later time by the massive stars. However, this prediction is exactly opposite to the empirical conclusions reported above for U Sco.

How might we approach the inconsistency between the ages of stars of different masses in U Sco? To get guidance in this regard, we consider it worthwhile to consider the case of another young association: the β Pic moving group (BPMG).

1.3. The case of BPMG

The moving group associated with the star β Pictoris has been the subject of many investigations of its age. The range of ages which various researchers have reported is rather wide (factor of at least 2.5, and possibly as large as 5). For present purposes, it is pertinent to note that the lower end of the age range of BPMG overlaps the upper end of the age range of U Sco. Therefore, in order to set the stage for the present paper, it is relevant to mention how a consistent interpretation of certain empirical information about stars in the BPMG has emerged in the context of a particular model of magneto-convection.

MacDonald & Mullan (2010) noted that isochronal and Li depletion age estimators give statistically significant differences in the ages of individual stars in the β Pic moving group. They proposed that the resolution of this discrepancy lay in the effects of inhibition of convective onset due to the presence of internal magnetic fields in the BPMG stars. The inhibition of convection by internal magnetic fields has the effect of slowing down the process of contraction of pre-main sequence stars towards the main sequence. Since the process of pre-main sequence contraction causes the star to move downward and to the left in the HRD, the slowing down of contraction by magneto-convective processes has the effect that magnetic stellar models with a given age, are found to be larger and cooler than non-magnetic models of stars with the same age.

In the present paper, our goal is to apply our magneto-convective model to interpret the empirical properties of four low-mass stars in U Sco.

We note that Feiden (2016) has also recently applied a different model of magneto-convection to two of the low-mass stars which we propose to model in U Sco. We will compare our results with Feiden's in the Discussion (Section 6, below).

2. The important role of eclipsing binaries in more stringent testing of models of stellar evolution

Double line eclipsing binaries provide masses and radii for stars with higher precision than any other method (Torres, Andersen & Gimenez, 2010). If the stellar age and composition are also well constrained, these measurements provide stringent tests of stellar evolution models. For a number of short period binaries with M star components, it has been found that standard stellar evolution models predict radii for the stars which are significantly smaller than the empirical radii. That is, empirical radii indicate that the stars are “oversized” (“bloated”) relative to the model predictions. Examples among solar neighborhood stars are YY Gem (Torres & Ribas 2002) and CM Dra (Morales et al 2009). For both systems, the radius excess is at least a 5σ effect when compared to the (small) statistical errors. A third system is CU Cnc (Ribas 2003) for which evolutionary models underestimate the stellar radii by as much as 10%.

Since all three of the above binaries show evidence for magnetic activity (flares and spots) an attractive explanation for the oversizing is that it is due to the presence of an internal magnetic field. The magnetic field leads to increased radius either because of magnetic inhibition of convective onset (Mullan & MacDonald 2001) or the presence of surface dark spots (Chabrier, Gallardo, & Baraffe 2007) or a combination of the two.

MacDonald & Mullan (2014) applied a combined magnetic inhibition and spot model to the stars in these 3 binary systems and determined surface magnetic field strengths (ranging from 320 to 560 G) in good agreement with the magnetic fluxes which can be derived from the empirical X-ray luminosity–magnetic flux relation (Pevtsov et al. 2003; Feiden & Chaboyer 2013).

In the 3 short period binaries in the solar neighborhood discussed by MacDonald and Mullan (2014), the stars experience strong dynamo action because of tidal locking of axial rotation to the (short) orbital period. However, in the case of U Sco, the stars are young enough that magnetic braking has not had enough time to remove significant angular momentum. As a result, the stars in U Sco are expected to have a distribution of rotation rates and a range of surface magnetic field strengths arising from dynamo action. This leads us to expect that some fraction of the USco cluster members may be “oversized” due to magnetic effects. MacDonald & Mullan (2013) proposed this as an explanation of the finding by Jackson, Jeffries & Maxted (2009) that the mean radii for low-mass M-dwarfs in the (relatively) young, open cluster NGC 2516 (age = 125 ± 25 Myr) are larger than model predictions at a given absolute I magnitude or I – K color and also larger than measured radii of magnetically inactive M-dwarfs.

The reliable identification of red dwarfs with empirical radii which are definitely “oversized” relative to evolutionary predictions has become possible in recent years only because the precision with which stellar radii can be determined has improved to the point that the empirical uncertainties in radii are now better than a few percent. In the best cases, the uncertainty in radius is better than 1%. The latter case applies to two of the U Sco stars which we will attempt to fit in the present paper: the smallness of the errors in masses and radii constrain the permitted ranges of the magnetic parameters.

3. Precise empirical data for 2 eclipsing binaries in U Sco

In this section we summarize the properties of two binaries which are members of USco. In each of these binaries, the two components turn out to have nearly equal masses, but the stars in one binary are 3 times more massive than the stars in the second binary. In the more massive binary (USco5), the components have masses in the range 0.3-0.35 M_{\odot} : such stars are close to the boundary where theoretical models of stellar structure predict that main sequence stars undergo a transition to complete convection. However, in the course of pre-main sequence (and early main sequence) evolution, such stars may contain a radiative zone (RZ) for a more or less extended interval of time. In view of this, and in order to distinguish the USco binaries from each other, we shall refer for brevity to the components in USco5 as RZ stars. On the other hand, the less massive binary (EPIC 203710387) contains components with masses close to 0.1 M_{\odot} : such stars are completely convective (CC) at all stages of evolution. We shall refer to these components as CC stars.

3.1. Two RZ M dwarfs in USco: empirical data

UScoCTIO 5 (USco5) was discovered to be a low-mass spectroscopic binary system with orbital period 34 d by Reiners, Basri & Mohanty (2005). The components are both of spectral type M4.5. Membership of the Upper Sco OB association was first proposed by Ardila et al. (2000) and confirmed by Reiners et al. (2005) based on the detection of Li absorption lines. Kraus et al. (2015) showed that primary and secondary eclipses are apparent in the K2 extended *Kepler* mission light curves. From the existing radial velocity measurements of Reiners et al. (2005) and analysis of the light curve, Kraus et al. (2015) determine the component masses and radii to be $M_A = 0.329 \pm 0.002 M_{\odot}$, $R_A = 0.834 \pm 0.006 R_{\odot}$, $M_B = 0.317 \pm 0.002 M_{\odot}$, and $R_B = 0.810 \pm 0.006 R_{\odot}$. Note that the relative errors in both masses and radii are better than 1%.

Kraus et al. (2015) compared the location of the components in the HRD to a number of standard (non-magnetic) stellar evolutionary models and found that none of the evolutionary models gave satisfactory agreement with the observations. A detailed analysis (Pecaut, Mamajek & Bubar 2012) finds an age for the OB association of 11 ± 3 Myr. At this age, the models predict an effective temperature for the M dwarfs in USco5 of $T_{\text{eff}} \sim 3400$ K: this is higher than that determined from the spectral type, $T_{\text{eff}} = 3200 \pm 75$ K, a 2.5σ discrepancy. Equivalently, the empirical stellar radii for the M dwarfs in USco5 are greater than the model predictions by $\sim 10\%$.

An independent analysis of the USco5 K2 light curve by David et al. (2016) gives slightly larger masses $M_A = 0.3336 \pm 0.0022 M_{\odot}$, $M_B = 0.3200 \pm 0.0022 M_{\odot}$ but significantly greater radii $R_A = 0.862 \pm 0.012 R_{\odot}$, $R_B = 0.852 \pm 0.013 R_{\odot}$. Note that in these cases, although the masses are still determined to better than 1%, the radii are now determined with somewhat poorer precision. Nevertheless, even the errors in the radii are still not much larger than 1%, and therefore present a challenge to attempted model fits.

3.2. Two CC M dwarfs in USco: empirical data

David et al. (2016) also reported the discovery of three new low-mass double-lined eclipsing binaries in the Upper Scorpius association. Of these three, one contains a G star and a K star, and one contains two brown dwarfs: in the present paper, where we are interested in M dwarfs, we will not discuss these two systems. But the third system (EPIC 203710387), containing nearly identical CC M dwarfs, is of interest to us. David et al. (2016) have determined masses and radii as follows: $M_A = 0.1183 \pm 0.0028 M_{\odot}$, $M_B =$

$0.1076 \pm 0.0031 M_{\odot}$ and $R_A = 0.417 \pm 0.010 R_{\odot}$, $R_B = 0.450 \pm 0.012 R_{\odot}$. For these stars, the errors in masses and radii are not quite as good as for the components of USco5: nevertheless, with errors in the 2-3% range, the data of David et al. (2016) are certainly adequate to offer challenges to obtaining good fits between data and stellar models.

A noteworthy feature of the empirical data reported by David et al. for the CC stars in USco is this: of the two stars in the binary, the *lower* mass star is found to have the *larger* radius. This is reminiscent of the unusual case of another pair of young stars where the lower mass component was observed to be hotter than the higher mass component (Stassun et al. 2007). Standard evolutionary models *cannot* explain the existence of a larger radius in the lower mass component if the two components are coeval. In our view, a possible resolution of this discrepancy is that the lower mass star has a stronger magnetic field than the higher mass component: the presence of a stronger field in the low mass component gives rise to the radius inversion. (An analogous resolution of the “surprising” temperature inversion reported by Stassun et al. [2007] has been reported by MacDonald & Mullan [2009].)

3.3. Exploration of magnetic effects on either side of the transition from RZ to CC

The pairs of low mass U Sco stars which we study in this paper probably lie on opposite sides of the RZ/CC divide. It is possible that there are physical differences in the ways in which the structure of a star responds to magnetic fields depending on whether it is RZ or CC. In view of this, an advantage of studying structural magnetic effects in stars which are known to be members of the same association, is that it might be easier to detect such structural differences (if there are any) by studying stars in which one of the crucial parameters of stellar evolution is held fixed, namely, the age.

4. Code and models

Our code has already been described in MacDonald & Mullan (2012, 2013, 2014). Here we note only some comments which are necessary to set the stage for the present application of the code.

4.1. Boundary conditions: three approaches

We start by calculating 3 standard (i.e. non-magnetic) models of the evolution of a star with a given mass using three approaches to the boundary conditions (see Mullan et al. 2015). For all 3 models, we use the SCVH+Z equation of state, which is constructed by adding the contribution from heavy elements to the hydrogen – helium equation of state of Saumon, Chabrier & Van Horn (1995). The 3 models (which we refer to as belonging to Sets A, B, and C) differ in the way we select (a) the mixing length, and (b) the outer boundary condition. For set A, we use a mixing length ratio, $\alpha = 1.7$. This is the value of α which best fits the observed properties of the current Sun. In Set A, the outer boundary conditions on temperature and pressure are determined by applying the Eddington approximation at optical depth 0.1. The modelling of set B is the same as for set A except that we use $\alpha = 1.0$. This choice of mixing length ratio is used for ease of comparison with our third set of models, Set C. For Set C the outer boundary conditions on temperature and pressure are set by their values at the base of BT-Settl atmosphere models (Allard, Homeier & Freytag 2012, Allard et al. 2012, Rajpurohit et al. 2013) at optical depth 10^3 . We use $\alpha = 1.0$ for consistency with the actual value of the mixing length ratio which was used in the calculation of the BT-Settl atmosphere models.

In Figures 1-3 below, we will present the results we have obtained for the evolutionary track of radius R and T_{eff} in the pre-main sequence phase of evolution for the RZ stars (USco5). In Figures 4-6, we will

present analogous tracks for our chosen 2 CC stars in USco. In all cases, the first step in our work will be to calculate standard (non-magnetic) evolutionary models starting from a fully convective Hayashi phase model of high luminosity. To provide guidance for the evolutionary time-scales, each figure will include three isochrones to demonstrate how long it takes for a star to move along a track: the isochrones (which will appear as nearly horizontal lines in Fig. 1-6) are plotted for ages in Myr of 8 (upper line), 11, and 14 (lowest line). In Figures 1-3, which refer to stars with masses of about $0.3 M_{\odot}$, small “hooks” can be seen near the bottom of each curve: these indicate the approach to the main sequence. In Figures 4-6 (for stars with masses of about $0.1 M_{\odot}$), the hooks are absent: the reason for this is that the plotted results span a range of times which are too short for the low-mass CC stars to reach the main sequence.

In Figures 1-6, the left-most evolutionary track will indicate the results which we have obtained for non-magnetic models. These can be used as fiducial tracks so that the reader can appreciate the changes that occur when a non-standard (magnetic) model with the same mass is eventually computed. Inspection of Figures 1-6 indicates that the fiducial tracks are in all cases inconsistent with the empirical values of R and T_{eff} .

In order to extend models in Sets A and B to include magnetic effects, our approach is based on a physics-based treatment of magnetic inhibition of convective onset (see Section 4.1 below). The tracks obtained for various magnetic models of this kind are plotted in Figs. 1, 2, 4, and 5. We will find that the larger the field, the cooler the models, i.e. the more the corresponding evolutionary track is displaced towards the *right-hand* side of the plot.

However, in the case of Set C models, we do not model magnetic effects in terms of convective inhibition. Instead, we take a different approach: we model the effects of magnetic fields by imposing dark spots which occupy a certain fraction of the stellar surface. Set C is used to determine the degree of surface spot coverage needed to reconcile measured and calculated stellar surface properties.

4.2. Magnetic inhibition model

Our magnetic inhibition model is based on work of Gough & Tayler (1966; hereafter GT), who derived a criterion for the onset of convective instability in the presence of a magnetic field based on an energy principle which is widely used in plasma physics applications (Bernstein et al. 1958). The original GT criterion depended on a single magnetic inhibition parameter, δ . However, when the criterion is applied to stars, the introduction of a second parameter is also advisable: an upper limit, or “ceiling”, on the magnetic field strength, B_{ceil} (MacDonald & Mullan 2012). An important aspect of our “two-parameter” solutions is noteworthy: our magnetoconvective best-fit solutions for any given star are much more sensitive to the value of the parameter δ than to the value of B_{ceil} . This allows us to determine the best fit value of δ within uncertainties which are no worse than 10’s of percent even when the allowed values of B_{ceil} may be spread over several orders of magnitude. The significance of this aspect has been stressed by MacDonald & Mullan (2014): “despite the broad range of uncertainty in the *deep interior* field strengths, this does *not* translate ...into an equally broad range of *surface* field strengths.....our predictions of the surface field are subject to observational test, even if the $B_{ceiling}$ values are not”.

According to GT, the magnetic inhibition of convective onset is modelled by modifying the usual Schwarzschild criterion for convective onset to become

$$\nabla > \nabla_{ad} + \Delta, \quad (0.1)$$

Here, ∇ and ∇_{ad} are the structural and adiabatic logarithmic temperature gradients with respect to pressure, and

$$\Delta = \frac{\delta}{\theta_e}, \quad (0.2)$$

where $\theta_e = -\partial \ln \rho / \partial \ln T|_p$ is a dimensionless thermal expansion coefficient.

In the original GT criterion, which is derived under the assumption that ideal gas conditions prevail, δ is related to the vertical component of the magnetic field, B_v , and the gas pressure, P_{gas} , by

$$\delta = \frac{B_v^2}{B_v^2 + 4\pi\gamma P_{gas}}, \quad (0.3)$$

where γ is the first adiabatic exponent. The modification in equation (0.2) compared to the original GT criterion is made in order to take into account non-ideal gas effects (MacDonald & Mullan 2009).

In general, δ may vary as a function of the radial position in a star. Based on dynamo concepts (MacDonald & Mullan 2012), we take δ to have a constant numerical value from the surface down to the radial location at which the local magnetic field strength reaches B_{ceil} . At deeper radial locations, the field is held fixed at B_{ceil} . In the models used here, we set $B_{ceil} = 1$ MG: this is the largest value of the equilibrium field strength which has been found to occur in a rotationally-driven interface dynamo in early M dwarfs (Mullan et al 2015).

To determine the convective energy flux in our magnetic models, we replace ∇_{ad} by $\nabla_{ad} + \Delta$ everywhere it appears in the mixing length theory for convection.

4.3. Spot model

Certain low-mass stars are known to have dark spots which are present temporarily on their surface (e.g. Kron 1952). These dark spots, which can have areas as large as 20% of the visible stellar hemisphere (e.g. Bopp & Evans 1973), temporarily block a significant fraction of the outward energy flux which wells up from the deep interior of the star. If enough flux is blocked at the surface, the stellar parameters such as R and T_{eff} are expected to adjust in order to handle the internal redistribution of flux. In our work, the approach to including the blocking effects of surface dark spots is based on work by Spruit & Weiss (1986) and Spruit (1992): see MacDonald & Mullan (2012, 2013) for a description of our approach. In this model, there is a single additional parameter, f_s , the effective fraction of the surface covered by spots, which are assumed to be completely dark. The surface boundary condition is then

$$L = 4\pi R^2 (1 - f_s) \sigma T_u^4, \quad (0.4)$$

where T_u is the surface temperature of the immaculate (unspotted) surface, which is set equal to the model temperature at optical depth $2/3$.

Note that in modeling the presence of dark spots on the surface of a low-mass star in this way, no assumption whatsoever is made about the operation of magnetic effects in the spots: it is simply assumed that (for unspecified reasons) a completely dark patch with a certain area exists on the star's surface. In

view of this assumption, there is no direct method of using the size of a dark spot on a star to estimate the strength of the magnetic field which might (by analogy with sunspots) be present. Indirect methods might be devised to estimate the field (e.g. see Section 5.1 below), but too many unknown parameters are involved to allow reliable estimates.

4.4. Estimation of fit parameters

To determine best fit parameters and their standard deviations, we use a Monte Carlo method. We assume that the mass, radius and T_{eff} of each star are distributed in Gaussian form over a range of values on either side of the mean value. By interpolation in the model grids, we find the age and e.g. magnetic inhibition parameter values that match best the empirical radius and T_{eff} . The mean and standard deviation of a fit parameter are determined from 100,000 trials.

5. Results

We have applied our models to the observations of the RZ and CC stars in USco. Since the stellar radii have very small uncertainties, the luminosity and effective temperature are highly correlated. Hence, instead of plotting our results in the traditional HRD, we find it more instructive to use a diagram in which the radius R is plotted against effective temperature T_{eff} . Kraus et al. (2015) and David et al. (2016) have both relied on spectral types and flux ratios to determine T_{eff} .

5.1 The RZ system in USco

Since the components of USco 5 are very similar, instead of plotting the components individually, we have modelled the mean of the two objects as a single track in Figures 1-3.

In Figure 1, we compare the location of the “mean” USco5 in the R - T_{eff} diagram with evolutionary tracks of magnetic models from set A for mass, $M = 0.32 M_{\odot}$. Each magnetic track corresponds to a field with a particular value of δ , ranging from 0 (the standard model: left-most track in Fig. 1) to 0.06 (the right-most track in Fig. 1). The rectangle with the solid border shows the position of the mean component using the results of Kraus et al. (2015). The rectangle with the dashed border shows the position of the mean component using the results reported by David et al. (2016). With the results plotted in Fig. 1, we find that the best fit between our magnetic tracks and the empirical data for the “mean” component occurs for $\delta = 0.039 \pm 0.008$. Also shown in Fig. 1 are isochrones for ages 8, 11 and 14 Myr. Our fitting technique also gives a value for the age of the magnetic model which best fits the empirical R and T_{eff} . The observational constraints of Kraus et al. (2015) allow us formally to compute slightly different tracks for the two components of USco5: the best formal fits are obtained for ages of 10.5 ± 0.9 Myr for U Sco5 A and 11.3 ± 1.0 Myr for U Sco5 B. For the observational constraints of David et al. (2016), we obtain ages of 9.9 ± 2.0 Myr for U Sco5 A and 10.6 ± 2.0 Myr for U Sco5 B. For the A component, $\delta = 0.040 \pm 0.015$ and for the B component, $\delta = 0.042 \pm 0.014$. Clearly, these estimates of ages and best-fit δ values are so close to each other for the two components of USco 5 that there is no statistically significant difference between them. This justifies our use of plotting only a single set of tracks for USco5 A and USco5 B in Fig. 1. The best-fit values of δ for USco5 (according to models belonging to Set A) correspond to surface values of B_V in the range 320 – 470 G.

Figure 2 is the same as Figure 1 except that the models are from set B. Agreement with the observational constraints of Kraus et al. (2015) are obtained for ages 10.8 ± 0.9 Myr for U Sco5 A and 11.6 ± 1.0 Myr

for U Sco5 B. For both components, $\delta = 0.030 \pm 0.008$. For the observational constraints of David et al. (2016), we obtain ages 10.2 ± 2.0 Myr for U Sco5 A and 10.8 ± 2.0 Myr for U Sco5 B. For the A component, $\delta = 0.031 \pm 0.016$ and for the B component, $\delta = 0.034 \pm 0.015$. As before, we note that there are no statistically significant differences between ages and best-fit δ values for USco5 A and USco5 B. The predicted range in B_V (according to models belonging to Set B) is 230 – 420 G.

Turning now to models belonging to Set C, we show in Figure 3 a comparison between the location of USco5 in the $R-T_{eff}$ diagram and the location of evolutionary models containing dark spots for a range of values of the fractional areal coverage f_s . Agreement with the observational constraints of Kraus et al. (2015) are obtained for age 10.0 ± 0.9 Myr for U Sco5 A and 10.8 ± 1.1 Myr for U Sco5 B. For both components, the best fit models have $f_s = 0.33 \pm 0.06$. For the observational constraints of David et al. (2016), we obtain ages of 9.6 ± 2.1 Myr for U Sco5 A and 10.4 ± 2.2 Myr for U Sco5 B. For the A component, $f_s = 0.35 \pm 0.15$ and for the B component, $f_s = 0.34 \pm 0.14$. Once again, there are no statistically significant differences between the results for USco5 A and USco5 B.

In the case of Set C, there is no obvious way to predict the surface magnetic field strength which corresponds to a given fractional areal spot coverage, unless one makes several assumptions. E.g. Bopp & Evans (1973) suggest that the magnetic field strength in a starspot can be calculated if one knows the following information: the thickness of the spherical shell where energy is trapped, the efficiency with which the radiative flux deficit is converted into magnetic energy, and the length of time during which the flux deficit is stored in magnetic energy before being released in a flare. For lack of information concerning these factors in the RZ and CC stars in USco, we do not make any estimates in this paper concerning magnetic field strengths in Set C models.

We draw attention to an important quantitative conclusion that can be inferred from Figs 1-3. Whether we use boundary conditions from Sets A, B, or C, the ages which emerge from our best-fit magnetic models of the RZ stars in USco5 are found to lie in the range 9.6 ± 2.1 to 11.6 ± 1.0 Myr. These results are consistent with the ages obtained for the more massive stars in USco: 11 ± 3 Myr (as described in Section 1.2 above).

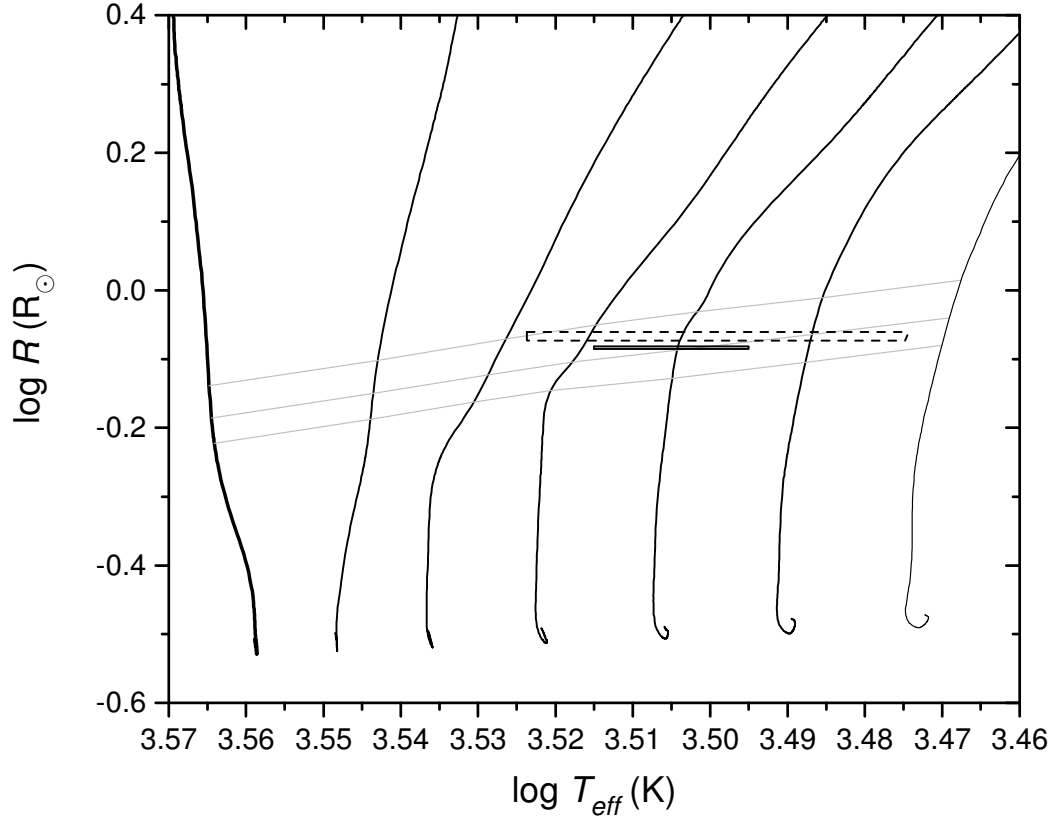


Figure 1. Comparison of the location of RZ system USco5 in the $\log T_{\text{eff}} - \log R$ diagram with models for which we use boundary conditions belonging to set A (see Section 4.1) for $M = 0.32 M_{\odot}$. The magnetic inhibition parameter ranges from 0 (leftmost track: non-magnetic “standard evolution”) to 0.06 (rightmost track) in increments of 0.01. The rectangles show the position of the mean component using the results of Kraus et al. (2015, solid border) and David et al. (2016, dashed border). Also shown are isochrones for ages 8, 11 and 14 Myr.

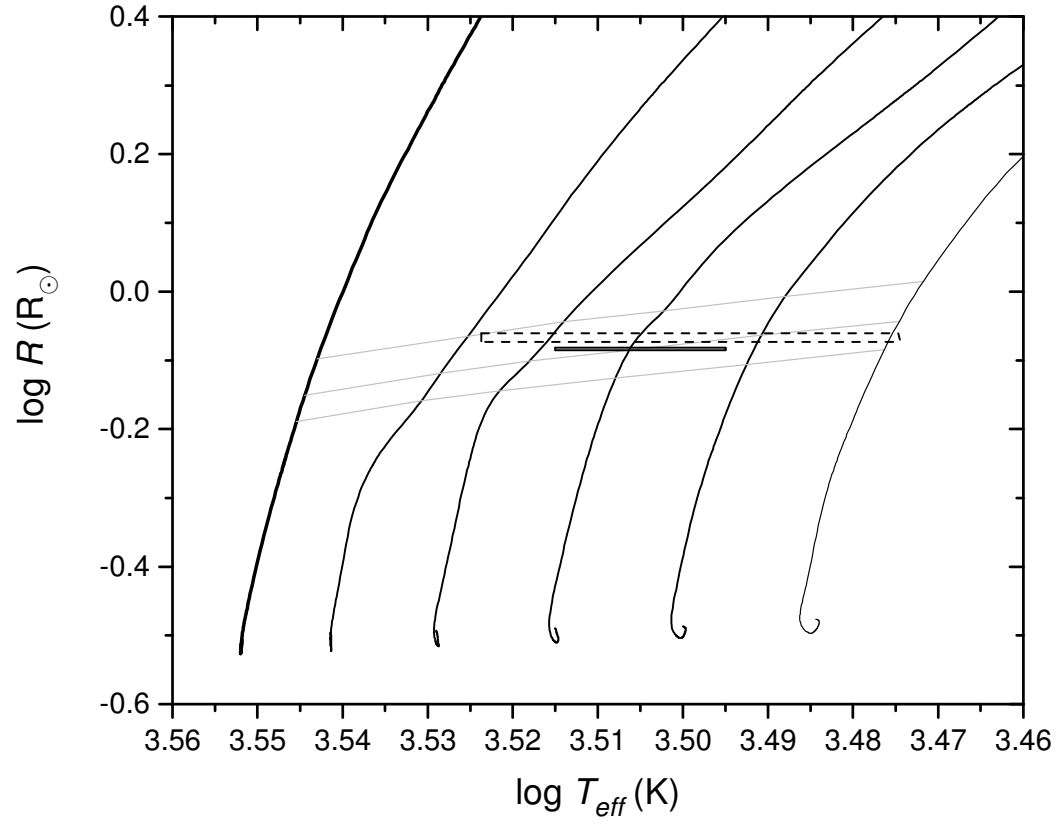


Figure 2. Analogous to Figure 1, except for models of the RZ system USco5 for which we use boundary conditions belonging to set B (see Section 4.1). Here, the magnetic inhibition parameter ranges from 0 (leftmost track) to 0.05 (rightmost track) in increments of 0.01.

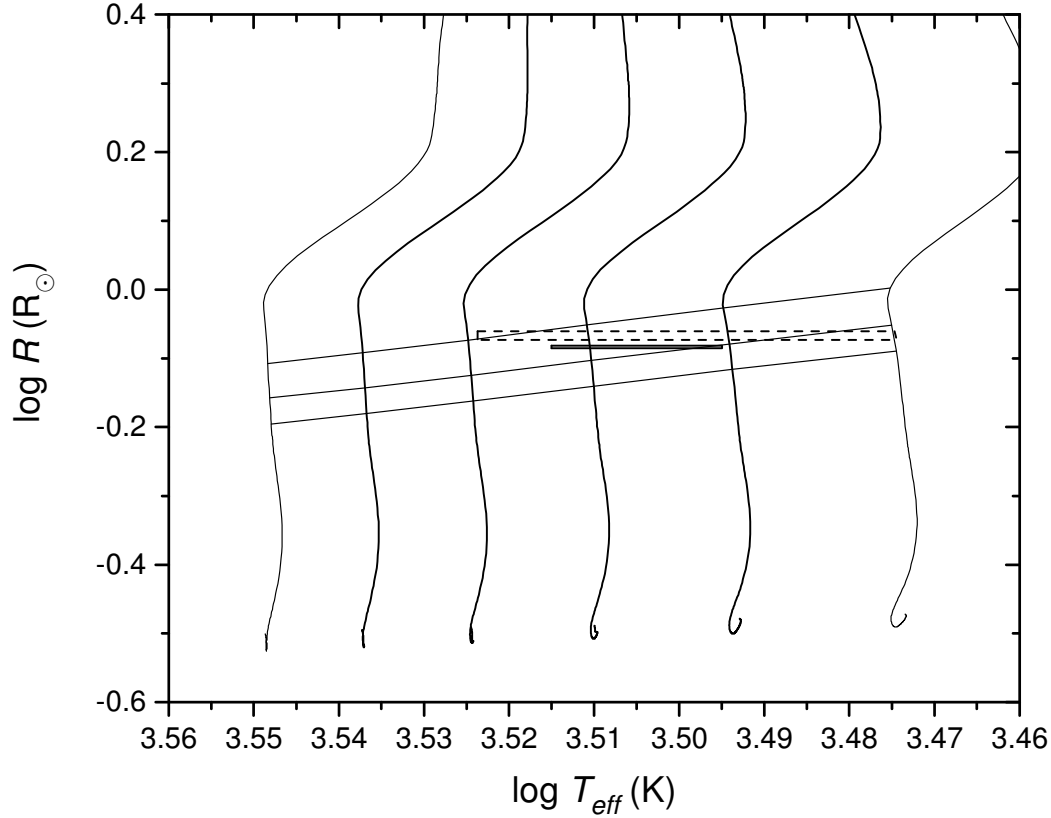


Figure 3. Analogous to Fig. 1, except for models the the RZ system USco5 for which we use boundary conditions belonging to set C (see Section 4.1) for $M = 0.32 M_{\odot}$. Here, the spot coverage parameter ranges from 0 (leftmost track: “standard evolution”) to 0.5 (rightmost track: heavily spotted) in increments of 0.1.

5.2 The CC system in U Sco

In Figure 4, we show pairs of evolutionary tracks in the $R - T_{eff}$ diagram which are obtained for models of mass 0.12 (red lines) and 0.11 (blue lines) M_{\odot} when we use boundary conditions belonging to set A (see Section 4.1). The long rectangular boxes show the empirical locations of E2037 A (red) and E2037 B (blue). Also shown are isochrones. If we were to attempt to interpret the empirical parameters in terms of non-magnetic models (as plotted on the leftmost pair of tracks), the empirical radii of the two components would require ages of 9.03 ± 0.54 Myr for E2037 A and 7.35 ± 0.53 Myr for E2037 B. According to this interpretation, the two components of the CC system cannot be coeval: they differ in age by about 2σ . An additional difficulty with the nonmagnetic model interpretation is that the models would predict effective temperatures for both components that are ~ 300 K higher than the empirical values.

However, when we consider magnetic models, the ones which fit the empirical values best (by passing closest to the centers of the rectangular boxes) are found to have ages of 12.8 ± 1.4 and 12.6 ± 1.6 Myr for components A and B, respectively. These ages are consistent with coevality for the components. As regards the best fit models, the magnetic inhibition parameters are found to have the values $\delta = 0.027 \pm 0.006$ and 0.038 ± 0.006 . Combining these values of the best-fitting δ with the surface gas pressure in the

RZ models (according to eq. 1.3), the corresponding surface vertical field strengths are found to be 340 – 430 G in component A and 420 – 500 G in component B. Why does the field turn out to be stronger in component B? The reason is that the oversizing of component B is definitely more extreme than in component A. To see this, note that if standard evolution of coeval components were to be applicable, component B should be smaller than component A. Specifically, at a particular age (e.g. 8 Myr), the red isochrone in Fig. 4 intersects the leftmost red track at a radius of $\log R = -0.333$, while the blue isochrone at the same age intersects the leftmost blue track at $\log R = -0.365$. Thus, standard evolution predicts that component B should have a radius which is 7-8% *smaller* than the radius of component A. (Similar quantitative differences are also found if we examine where the isochrones for 11 and 14 Myr intersect the leftmost tracks.) However, in fact, the empirical radii (David et al. 2016) show that component B is *not* smaller than component A. Instead, the opposite is the case: component B is found to have a radius which is 7-8% *larger* than component A. Thus, relative to the “standard” evolutionary tracks, the empirical oversizing of component B is more extreme than the oversizing of component A. This has the effect that, when we attempt to interpret the empirical data in terms of a magnetic model, a stronger magnetic field is required to fit the empirical radius in component B.

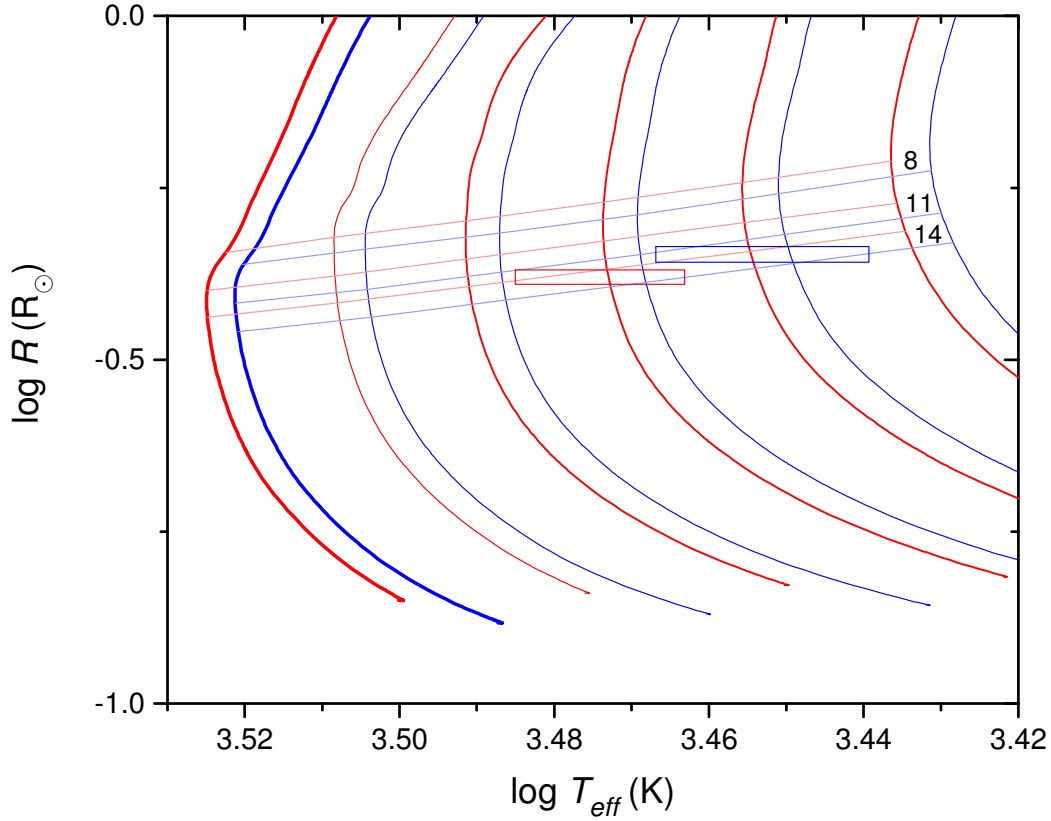


Figure 4. Comparison of the locations of the CC stars in USco (E2037A and B) in the $R - T_{\text{eff}}$ diagram with models for which we use boundary conditions belonging to set A (see Section 4.1) for $M = 0.12 M_{\odot}$ (red) and $0.11 M_{\odot}$ (blue). The magnetic inhibition parameter ranges from 0 (leftmost tracks: nonmagnetic “standard evolution”) to 0.05 (rightmost tracks) in increments of 0.01. The rectangles show the positions of component A (red) and B (blue) using the results of David et al. (2016). Also shown are isochrones for both masses at ages 8, 11 and 14 Myr.

Figure 5 is analogous to Figure 4 except the models are obtained by applying boundary conditions from set B. Because of the smaller convective efficiency in set B models (resulting from a shorter mixing length $\alpha=1.0$, rather than $\alpha=1.7$ in set A), the radii in set B models, even in the non-magnetic limit, are already systematically larger than those in set A models. The difference in radii can be quantified by comparing the location of the intersection of (say) the 8 Myr isochrones with the left-most red track: in Fig. 4, this occurs at $\log R = -0.333$, while in Fig. 5, it occurs at $\log R = -0.316$. That is, the nonmagnetic model from set B has a radius which exceeds the equivalent set A model by 4%. As a result, smaller fields suffice to give the oversizing that is needed to fit the empirical parameters. From the magnetic models, we find ages of 13.2 ± 1.5 and 13.0 ± 1.6 Myr for E2037 A and E2037 B, respectively. Once again, we note the advantage of using magnetic models: the components are found to be coeval. The values found for the magnetic inhibition parameter are $\delta = 0.020 \pm 0.006$ and 0.032 ± 0.007 . The corresponding surface vertical field strengths are 280 – 390 G and 380 – 470 G.

Figure 6 is analogous to Figure 4, except the models are obtained by using boundary conditions from set C. The spot models give ages of 13.0 ± 1.5 and 13.1 ± 1.7 Myr for E2037 A and E2037 B, respectively. The values found for the spot fraction parameter are $f_s = 0.22 \pm 0.07$ and 0.36 ± 0.07 . As was noted above for the RZ system, there is no obvious way to predict the surface magnetic field strength which corresponds to a given fractional areal spot coverage.

Also as regards the CC system in USco, we draw attention to a similar quantitative conclusion that can be drawn from Figs 4-6 as was drawn for the RZ system shown in Figs. 1-3. Whether we use boundary conditions from Sets A, B, or C, the ages which emerge from our best-fit magnetic models of the CC stars in USco5 are found to lie in the range 12.6 ± 1.6 to 13.2 ± 1.5 Myr. These results are consistent with the ages obtained for the more massive stars in USco: 11 ± 3 Myr (as described in Section 1.2 above).

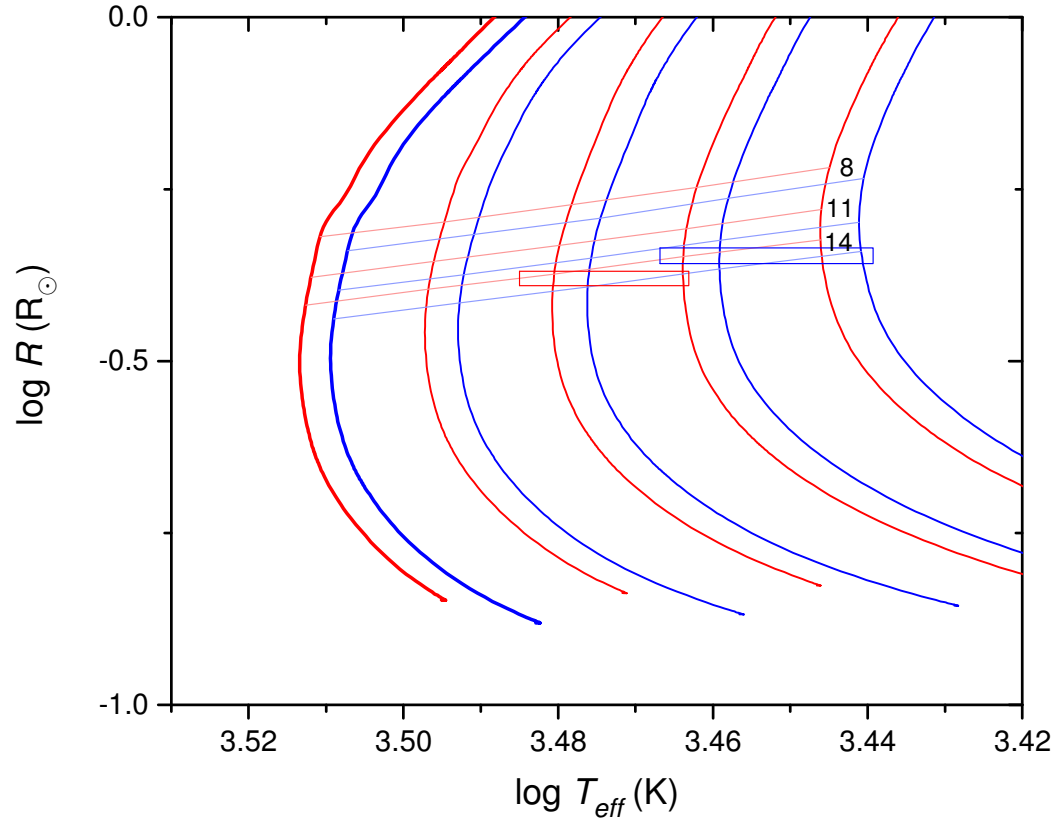


Figure 5. Analogous to Figure 4 except the models plotted here are those for which we use boundary conditions belonging to set B (see Section 4.1). The magnetic inhibition parameter ranges from 0 (leftmost tracks: nonmagnetic “standard evolution”) to 0.04 (rightmost tracks) in increments of 0.01.

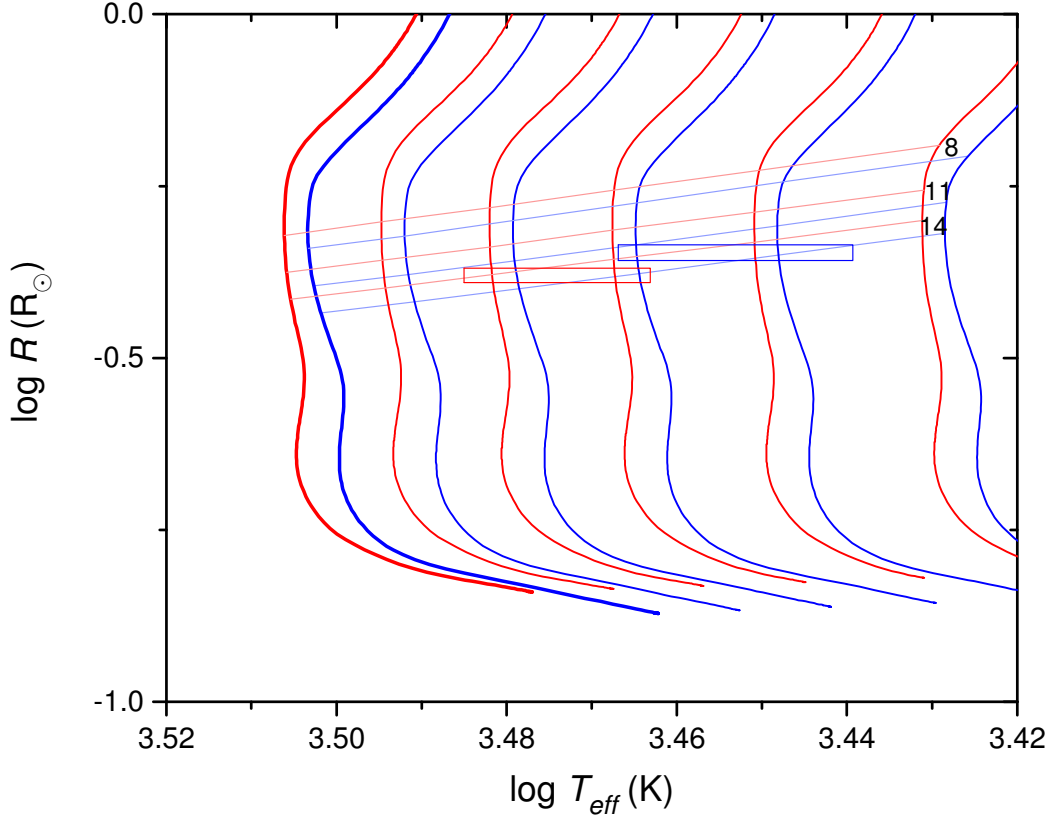


Figure 6. Analogous to Figure 4, except that the models plotted here are those for which we use boundary conditions belonging to set C (see Section 4.1). The spot coverage parameter ranges from 0 (leftmost track: unspotted “standard evolution”) to 0.5 (rightmost track) in increments of 0.1.

6. Discussion

6.1. Best-fit estimates of “age(s)” of U Sco stars: coevality restored

It might be expected that stars which are completely convective could respond to the presence of magnetic fields in a way which is structurally different from the response of stars which contain radiative zones. After all, although magnetic fields are certainly expected to have direct effects on convective motions (e.g. by interfering with motions transverse to the field lines, thereby inhibiting the onset of convection), the same fields are not expected to have any significant direct effects on radiative transfer. We note that the 4 low-mass stars which we have studied in this paper may straddle the boundary between completely convective stars and stars which contain radiative zones. In this regard, it is worth examining our results to see if there is any evidence of such structural differences between our RZ stars and our CC stars.

According to the 3 distinct sets (Sets A, B, C) of magnetic/spotted evolutionary tracks which we have computed, we find that the best-fitting models (according to the most recent empirical data: David et al. 2016) to the components of the RZ system in USco have ages as follows: 9.9 ± 2.0 Myr and 10.6 ± 2.0 Myr (Set A), 10.2 ± 2.0 Myr and 10.8 ± 2.0 Myr (Set B), and 9.6 ± 2.1 Myr and 10.4 ± 2.2 Myr (Set C). Note that the age determinations are insensitive to the mixing length ratio, because of the degeneracy in

changing mixing length ratio and changing the magnetic inhibition parameter or spot fraction (see MacDonald & Mullan 2014). Our models suggest that the best-fit age for the RZ stars in USco is in the range 9.6-10.8 Myr, with error bars of about 2 Myr.

We also find that the best-fitting models for the components of the CC system in USco have ages as follows: 12.8 ± 1.4 and 12.6 ± 1.6 Myr (Set A), 13.2 ± 1.5 and 13.0 ± 1.6 Myr (Set B), and 13.0 ± 1.5 and 13.1 ± 1.7 Myr (Set C). Our models suggest that the best-fit age for the CC stars is in the range 12.6-13.2 Myr, with error bars of about 1.7 Myr.

Thus, the 4 low-mass stars we have studied in USco are found to have ages in the range 9.6-13.2 Myr, with a mean value of 11.4 Myr. Combining the errors on our RZ stars and our CC stars, the error bars on this result are about ± 3 Myr.

We note that our results for the ages of magnetic models of 4 low-mass stars in USco overlap very well with the age determination of 11 ± 3 Myr reported for more massive stars in USco (with spectral types B, A, G, as well as Antares) by Peca et al. (2012). As a result, the “problem” of non-coevality in USco is resolved by our magneto-convective models.

6.2. Differences between magnetic models of RZ and CC stars?

Formally, the range of ages we have obtained for best-fit models of RZ and CC stars in USco are different: 9.6-10.8 Myr versus 12.6-13.2 Myr. This difference might contain a hint that the best-fit age to the RZ stars are younger than the best-fit age to the CC stars by an interval of order 3 Myr. If this discrepancy were to be statistically significant, it might provide evidence that a star with a radiative zone responds to magnetic fields in a structurally different way from a completely convective star.

In this regard, it is worth noting that recent results from Zeeman-Doppler imaging of young solar-type stars (Folsom et al. 2016) indicate that as a radiative zone develops in solar-type stars on the late pre-main sequence, changes in magnetic strength and geometry are “primarily driven by structural changes in the stellar interior”. Although the Folsom et al. study deals with stars having masses in the range $0.7-1.2 M_{\odot}$, and is therefore not directly applicable to the low-mass stars we study in USco, nevertheless, the study raises the possibility that differences in magnetic properties might occur also in our low-mass stars at the RZ/CC transition.

However, the statistical significance of the difference in the best-fit ages to our RZ stars and our CC stars is small: with errors of 2 Myr (RZ) and 1.7 Myr (CC), the formal difference in the age ranges corresponds to a statistical difference which is less than 1σ . As a result, we cannot yet conclude that the present results are an extension of the results of Folsom et al. towards lower masses.

6.3 Predictions of surface magnetic field strengths

Our models indicate that the strengths of the vertical component of the magnetic field at the stellar surface in the case of our best fit models for USco range from 230 to 470 G for the two RZ stars, and from 280 to 500 G for the two CC stars. Surface fields of comparable magnitude have previously been reported when we applied our magneto-convective model to three low-mass solar neighborhood binaries YY Gem, CM Dra and CU Cnc (MacDonald & Mullan 2014). Although the stars in the latter 3 systems are certainly not as young as the stars in U Sco, nevertheless the results are pertinent to the present discussion because the masses of the various components once again span the range of masses from RZ to CC. Thus, at 0.21 and $0.23 M_{\odot}$, the components of CM Dra are definitely in the CC class, whereas at $0.60 M_{\odot}$, each component

in YY Gem is definitely in the RZ class. The components of CU Cnc, at 0.40 and 0.43 M_{\odot} , are also in the RZ class.

In contrast to the approach we adopt here to model magnetoconvection in stars, Feiden & Chaboyer (2012, 2013) have used a fundamentally different approach to modelling the effects of magnetic fields on stellar structure and evolution. Feiden & Chaboyer (2013) report that a surface magnetic field strength of ~ 4 kG is required to replicate the empirical radii of the components of YY Gem. When MacDonald & Mullan (2014) applied their model to YY Gem, they found that the vertical component of the surface magnetic field is required to be in the range 320 – 350 G.

Recently, Feiden (2016) has applied the Feiden-Chaboyer model in order to address the age discrepancy in U Sco between high-mass and low-mass stars. Feiden’s derived a consistent age of 10 Myr for high- and low-mass stars in U Sco. In order to obtain this age for the low-mass stars, Feiden did not allow the surface field strength in a model of a low mass star in U Sco to be a floating parameter to be determined by fitting magnetic evolutionary tracks to the empirical data. Instead, in what he describes as a “critical” choice, Feiden prescribed the surface field strength to be equal *a priori* to the equipartition field strength B_{eq} in the gas at optical depth $\tau = 1$. For stars with a range of masses, this leads to surface fields of 0.76 kG in a 1.7 M_{\odot} star, and 2.64 kG in a 0.1 M_{\odot} star at an age of 10 Myr. Thus, for the low-mass stars we have discussed here, Feiden assumes a surface field of 2.44-2.64 kG in order to calculate his magnetic models of low-mass stars in USco. These strengths are to be compared with our own estimates of 230-500 G on the same stars.

We see that our estimates of surface field strengths in a field star as well as in U Sco stars are smaller than those of Feiden & Chaboyer by a factor which is at least as large as 5, and may be larger than 10.

Why is the difference in the estimates of field strengths so large between our models and Feiden’s? As regards the USco stars, the reason may be related to the fact that in the present paper, in contrast to Feiden (2016), our models do *not* prescribe the surface field strength *a priori*. Instead, a numerical value of δ is determined by best fits of evolutionary tracks to the empirical R and T_{eff} . Once a best fit value of δ has been determined, the surface field is calculated using eq. (1.3) above. In view of the definition of eq. (1.3), the small numerical values which we have obtained for δ ($=0.027$ - 0.042) in our USco stars are a quantitative expression of the fact that, at the stellar surface, our magnetic field estimates fall far below the equipartition value (for which $\delta = O(1)$). As a result, the Feiden values of surface field strengths in USco stars turn out to be significantly larger than ours.

6.4. Observational tests?

There are large differences between the surface field estimates of the Feiden model and the predictions of our model. This might mean that a direct measurement of the surface field strength in M dwarfs in U Sco or in solar neighborhood stars could help to discriminate between the two modelling approaches.

Observations of field properties in low mass stars have progressed greatly in recent years. Results from Zeeman-Doppler imaging (ZDI) allow observers to reconstruct in principle the three components of the magnetic field vector on a stellar surface in spherical coordinates, i.e. radial, azimuthal, and meridional (Donati et al. 2003). It is in terms of these three components that ZDI researchers typically present their results for any given star. However, the magnetic results which can be extracted from the ZDI data are inevitably weighted by inhomogeneities in surface brightness, as well as by fractional occupation of magnetic fields: as a result, small active regions containing intense fields are not necessarily detectable by ZDI. In the context of dynamo theory, it is usual to discuss generation of poloidal and toroidal

components of the field. The relationship between the theoretical dynamo components and the empirical spherical components is as follows. The observed azimuthal component corresponds to toroidal fields. The observed radial component contains no toroidal field, but corresponds to the poloidal field at higher latitudes. The meridional component corresponds better to the poloidal component at low latitudes.

In order to compare the results of our modeling with the observations, it is important to note the following. The field for which our models yield information (once the magnetic inhibition parameter δ has been determined) is the vertical component B_v (see eq. 1.3). It can be argued (Mullan, MacDonald & Townsend 2007) that, among the components of the stellar magnetic field which can be derived from ZDI (toroidal, meridional, poloidal), the one which is most closely related to B_v is the poloidal field at higher latitudes. Therefore, we are especially interested in observational results concerning the poloidal (radial) field.

Morin et al. (2010) have reported on magnetic topologies in a sample of M dwarfs in the solar neighborhood. The masses extending from $0.8 M_\odot$ to $0.1 M_\odot$. The ages of these stars are not likely to be as young as U Sco, but since the sample overlaps in mass with the RZ and CC stars we study here, we consider a comparison to be of interest. For a sample of younger stars, we refer to the results of Folsom et al. (2016): the youngest stars in the sample are estimated to be about 20 Myr old i.e. within a factor of 2 of the age of U Sco.

In the context of the results obtained in the present paper, one aspect of the work of Morin et al. and of Folsom et al. is noteworthy. Among the lowest mass solar neighborhood stars (0.21 - $0.09 M_\odot$; Morin et al.), poloidal fields are found to be dominant: 73-99% of the magnetic energy is in poloidal form. And among the younger stars (Folsom et al.), 80% of the stars in the sample also have the majority of their magnetic energy in the poloidal field. This suggests that when we attempt to making comparisons between empirical fields and the B_v results we obtain in the present paper (from our best fit δ values), we will be in effect comparing to the empirical fields which can probably be measured with the greatest confidence, namely, those which contribute the most to the overall magnetic energy.

On the other hand, when we wish to make an appropriate comparison between empirical results and Feiden's estimates of field strengths on the stellar surface (i.e. ~ 2500 G), we will need instead to pay attention to a different measurement. In this case, the relevant measurement is $\langle B \rangle$, the global average strength of the (unsigned) large-scale magnetic field over the surface of the star, i.e. the magnitude of the magnetic vector averaged over the surface of the star. According to Folsom et al. (2016), the 15 young solar-type stars in their sample (with ages between 20 and 250 Myr) have $\langle B \rangle$ values in the range 13.9-139.6 G. Folsom et al also provide the values of the peak field strength measured by ZDI: for the 15 stars in their sample, the values B_{peak} range from 40.2 to 793.4 G. It does not seem that either range overlaps with Feiden's (2016) estimate of ~ 2500 G surface fields in the U Sco low-mass stars. On the other hand, one of the late M dwarfs observed by Morin et al. (GJ 51) is reported to have $\langle B \rangle = 1.6$ kG, which is not far from Feiden's estimate. However, among the other 5 late M stars reported by Morin et al., 4 with masses in the range 0.09 - $0.14 M_\odot$ are reported to have mean $\langle B \rangle$ values of 55 G, 90 G, 140 G, and 90 G. These are all significantly smaller than the equipartition value of 2.6 kG prescribed by Feiden as the surface field for stars with masses of $0.1 M_\odot$.

To compare with our own results, we need to compare our B_v values with the empirical poloidal field strength B_p . Folsom et al. have provided data for each young solar-type star for the fraction ϕ of the total magnetic energy which is in poloidal form. From this, we estimate an upper limit on the poloidal field

strength from $B_p \approx B_{peak} \sqrt{\phi}$. Using data from Folsom et al. for the 10 stars with the strongest fields, we find that the upper limits on B_p range from 162 to 619 G. This range overlaps well with our estimates of 230-500 G for the surface field strengths in the 4 low-mass stars in USco.

These comparisons should not be taken too literally: they involve solar neighborhood stars and stars in clusters which are all older than USco by factors of 2 or more. In order to have a reliable comparison between theory and observation, we must wait until observers actually obtain ZDI data for the 4 low-mass stars in USco.

7. Conclusion

The U Sco association has, in the past, been notable for claims that the ages of the high-mass stars are apparently much older than those of the low-mass stars. We have obtained magnetic models for 4 low-mass components of two binary systems which belong to the young U Sco association. One of the binary systems contains stars with masses in the range 0.3-0.35 M_\odot : such stars may contain a radiative zone during certain evolutionary stages. The second binary system contains stars which are in the range 0.10-0.12 M_\odot : such stars are expected to be completely convective in U Sco. The magnetic models that we have obtained are successful in fitting the empirical data on R and T_{eff} at ages which (within the error bars) are identical for all 4 low-mass stars. Significantly, the ages which we have found to provide the best fit to the low-mass stars are also consistent with previous (independent) estimates of the ages of the more massive stars in the association. As a result, all of the stars in the U Sco association can now be regarded as coeval provided that magnetic fields are present in (at least) the low-mass stars. (Fields in higher-mass stars are not expected to lead to significant alterations to standard evolution.)

We have obtained marginal evidence for a difference in age between USco stars which are completely convective and USco stars which may contain a radiative zone. In statistical terms, the difference is less than 1σ . If more precise data are obtained indicating that this difference is statistically significant, it could indicate that structural changes due to magnetism in completely convective stars are different from those in stars with radiative zones.

Although we would like to compare our theoretical results for USco stars with empirical information about magnetic fields, no data are available which would allow us to make a direct comparison. In lieu of direct data on the young low-mass USco stars, we have examined ZDI data which have been reported for low-mass stars in the solar neighborhood (Morin et al. 2010) and also for young solar-type stars (Folsom et al. 2016). We find that the range of vertical surface field strengths which we have estimated from best-fit magnetoconvective models of U Sco low-mass stars overlap well with the range of upper-limit poloidal field strengths reported in young solar-type stars.

References

- Allard, F., Homeier, D., & Freytag, B. 2012a, Roy. Soc. London Philos. Trans. Ser. A, 370, 2765
- Allard, F., Homeier, D., Freytag, B., & Sharp, C. M. 2012b, in EAS Pub. Ser. 57, eds. C. Reyl  , C. Charbonnel, & M. Schultheis, 3

Ardila, D., Martín, E., & Basri, G. 2000, *AJ*, 120, 479

Bopp, B. W. & Evans, D. S. 1973, *MNRAS*, 164, 343

Chabrier, G., Gallardo, J., & Baraffe, I. 2007, *A&A*, 472, L17

de Geus, E. J., de Zeeuw, P. T., & Lub, J. 1989, *A&A*, 216, 44

Donati, J.-F., Cameron, A. C., Semel, M. et al. 2003, *MNRAS*, 345, 1145.

Feiden, G. A. 2016, arXiv:1604.08036

Feiden, G. A., & Chaboyer, B. 2012, *ApJ*, 761, 30

Feiden, G. A., & Chaboyer, B. 2013, *ApJ*, 779, 183

Folsom, C. P., Petit, P., Bouvier, J., et al. 2016, *MNRAS*, 457, 580

Gough D. O., Tayler R. J., 1966, *MNRAS*, 133, 85

Herbig, G. H. 1962, *ApJ* 135, 736

Herczeg, G. J., & Hillenbrand, L. A. 2015, *ApJ*, 808, 23

Jackson, R. J., Jeffries, R. D., & Maxted, P. F. L. 2009, *MNRAS*, 399, L89

Kraus, A. L., Cody, A. M., Covey, K. R., et al. 2015, *ApJ*, 807, 3

Kron, G. E. 1952, *ApJ* 115, 301

MacDonald, J., & Mullan, D. J. 2009, *ApJ*, 700, 387

MacDonald, J., & Mullan, D. J. 2012, *MNRAS*, 421, 3084

MacDonald, J., & Mullan, D. J. 2013, *ApJ*, 765, 126

MacDonald, J., & Mullan, D. J. 2014, *ApJ*, 787, 70

Maeder, A. 1981a, *Astron. Astrophys.* 93, 136

Maeder, A. 1981b, *Astron. Astrophys.* 99, 97

Maeder, A. 1981c, *Astron. Astrophys.* 102, 401

Morales J. C. et al., 2009, *ApJ*, 691, 1400

Morin, J., Donati, J.-F., Petit, P., Delfosse, X., Forveille, T. & Jardine, M. M. 2012, *MNRAS*, 407, 2269

Mullan, D. J., Houdebine, E. R., & MacDonald, J. 2015, *ApJ Letters*, 810, L18

Mullan, D. J. & MacDonald, J. 2001, *ApJ*, 559, 353

Mullan, D. J., MacDonald, J., & Townsend, R. H. D. 2007, *ApJ*, 670, 1420

Pecaut, M. J., Mamajek, E. E., & Bubar, E. J. 2012, *ApJ*, 746, 154

Pevtsov, A. A., Fisher, G. H., Acton, L. W., et al. 2003, *ApJ*, 598, 1387

Preibisch, T., Brown, A. G. A., Bridges, T., Guenther, E., & Zinnecker, H. 2002, *AJ*, 124, 404

- Rajpurohit, A. S., Reylé, C., Allard, F., et al. 2013, A&A, 556, A15
- Reiners, A., Basri, G., & Mohanty, S. 2005, ApJ, 634, 1346
- Ribas, I. 2003, A&A, 398, 239
- Saumon, D., Chabrier, G., & Van Horn, H. M. 1995, ApJS, 99, 713
- Spruit H. C., 1992, in Byrne P.B., Mullan D. J., eds, Surface Inhomogeneities on Late-Type Stars. Springer-Verlag, Heidelberg, Germany, p. 78
- Spruit H. C., Weiss A., 1986, A&A, 166, 167
- Stassun, K. G., Mathieu, R. D., & Valenti, J. A. 2007, ApJ, 664, 1154
- Torres G., Andersen J., Gimenez A., 2010, A&AR, 18, 67
- Torres, G., & Ribas, I. 2002, ApJ, 567, 1140